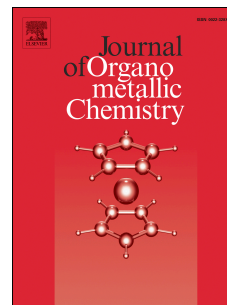


Accepted Manuscript

Characterisation and mechanistic study of the oxidative addition reactions of [Ir(cod)(sacac)]

Walter Purcell, Jeanet Conradie, S. Kumar, Johan A. Venter



PII: S0022-328X(15)30181-9

DOI: [10.1016/j.jorganchem.2015.10.012](https://doi.org/10.1016/j.jorganchem.2015.10.012)

Reference: JOM 19269

To appear in: *Journal of Organometallic Chemistry*

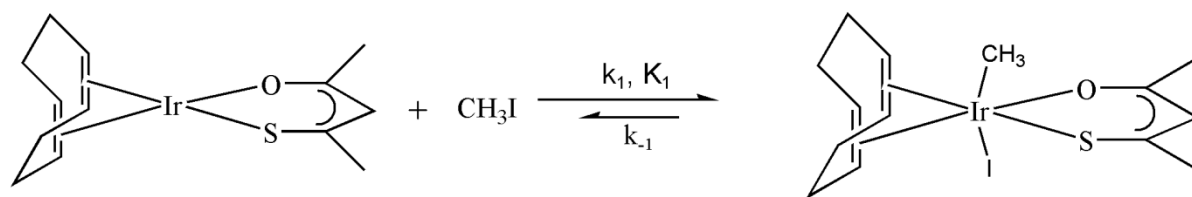
Received Date: 22 July 2015

Revised Date: 1 October 2015

Accepted Date: 6 October 2015

Please cite this article as: W. Purcell, J. Conradie, S. Kumar, J.A. Venter, Characterisation and mechanistic study of the oxidative addition reactions of [Ir(cod)(sacac)], *Journal of Organometallic Chemistry* (2015), doi: 10.1016/j.jorganchem.2015.10.012.

This is a PDF file of an unedited manuscript that has been accepted for publication. As a service to our customers we are providing this early version of the manuscript. The manuscript will undergo copyediting, typesetting, and review of the resulting proof before it is published in its final form. Please note that during the production process errors may be discovered which could affect the content, and all legal disclaimers that apply to the journal pertain.



ACCEPTED MANUSCRIPT

Characterisation and mechanistic study of the oxidative addition reactions of [Ir(cod)(sacac)]

Walter Purcell*, Jeanet Conradie, S. Kumar and Johan A. Venter

Department of Chemistry, PO Box 339, University of the Free State, Bloemfontein, 9300, South Africa.

Abstract

[Ir(cod)(sacac)] (sacac = thioacetyl acetonato) complexes were successfully synthesized and characterised using ^1H and ^{13}C NMR, IR and micro elemental analyses. The formation of isosbestic points in different solvents clearly indicate the formation of only one product, while the kinetic results for all of the complexes (except for chlorobenzene) showed simple second order kinetics with a zero intercept (within experimental error). The rate of oxidative addition showed little or no change with a solvent variation even with a large difference in polarity for the selected solvents, varying between 1.78×10^{-3} and $5.2(3) \text{ M}^{-1} \text{ s}^{-1}$ for chlorobenzene and acetonitrile respectively. Activation volumes were determined in four of the solvents, which varied between $+10.2(9)$ for chloroform to $-18(1) \text{ cm}^3 \text{ mol}^{-1}$ for acetonitrile. This solvent variation obeyed the Kirkwood equation with an intrinsic volume of activation of $-21(3) \text{ cm}^3$. A DFT analysis of the oxidative addition reaction shows that the *trans* addition is energetically favoured and that the *trans* [Ir(cod)(sacac)(CH₃)(I)]-alkyl product is more stable than the four possible *cis* [Ir(cod)(sacac)(CH₃)(I)]-alkyl products.

*Corresponding author, Fax: +27-(0)865255382, e-mail:purcellw@ufs.ac.za.

Key words: Iridium (I), thioacetyl acetonato ligand, cyclooctadiene, oxidative addition, high pressure kinetics, DFT

1. Introduction

Cyclooctadiene (cod) complexes of iridium(I) are mainly used as i) homogeneous catalysts in synthetic organic chemistry and ii) as starting material in the syntheses of other iridium organo-metallic complexes. One of the most well-known iridium (I) cod complexes is the Crabtree catalyst¹, $[\text{Ir}(\text{cod})(\text{PCy}_3)(\text{py})]\text{PF}_6$, (py = pyridine), which showed a 100 times increase in hydrogenation activity compared to the Wilkinson catalyst ($[\text{Rh}(\text{PPh}_3)_3\text{Cl}]$) and even allowed for the hydrogenation of tri and tetra substituted alkene. Consequently, the success of $[\text{Ir}(\text{cod})(\text{PCy}_3)(\text{py})]\text{PF}_6$ as a catalyst stimulated much research. This complex was used as the basis for the development of new catalysts in an attempt to modify its catalytic properties by selectively changing the bonded ligands to metal centre.^{2,3} The reaction of the $[\text{Ir}(\text{OMe})(\text{cod})_2]$ complex, in the presence of dipy catalyses the reaction between 1,2-dimethylbenzene and 1,2-di-*tert*-butyl-1,1,2,2-tetrafluorodisilane to yield 4-silyl 1,2-dimethylbenzene in yields of 99%.⁴ It was also found that different arenes and heteroarenes react with B_2pin_2 and HBpin in the presence of $[\text{Ir}(\text{cod})\text{Cl}_2]_2$ and bipyridine to produce the resulting aryl and heteroarylboron compounds.⁵ Other iridium cod complexes that exhibit catalytic properties are $[\text{Ir}(\text{cod})(\text{PPh}_3)_2]\text{OTf}$ ⁶, $[\text{Ir}(\text{cod})(\text{bzn})(\text{PR}_3)]^+(\text{bzn} = \text{benzotrile})$ ^{7,8}, $[\text{Ir}(\text{cod})(\text{PHOX})]^+$ (PHOX = phosphinooxazolidine, Pfaltz catalyst)⁹ and $[\text{Ir}(\text{cod})(\text{Pr}_2\text{PCH}_2\text{CH}_2\text{OMe})]\text{PF}_4$.¹⁰

The lability of the cod ligand renders the iridium cod compounds as ideal starting complexes for the synthesis of a variety of other iridium(I) complexes. For example, $[\text{Ir}(\text{biph})(\text{N}^{\wedge}\text{N})_2](\text{OTf})$ ¹¹ ($\text{N}^{\wedge}\text{N} = 2,2'$ dipyridyl or 4,4'-dimethyl-2,2' bipyridyl and $\text{Oft} = \text{CF}_3\text{SO}_3^-$) was synthesized from the $[\text{Ir}(\text{cod})(\text{bipy})\text{Cl}]_2$ dimeric complex, $[\text{Ir}(\text{Cl})(\text{CO})(\text{TPPTS})_2] \cdot x\text{H}_2\text{O}$ (TPPTS = *m*-trisulfonated triphenylphosphine) was prepared by substituting the cod ligand with CO in the presence of Cl^- ¹², as well as $[\text{Ir}(\text{cod})(\text{py})(\text{P}(\text{C}_6\text{H}_4-4-\text{OMe}_3))]\text{PF}_6$ ¹³ and $[\text{Ir}(\text{cod})(\text{ppol})]$ ¹⁴ (ppol = $\text{Ph}_2\text{PCH}_2\text{CH}_2\text{CH}_2\text{P}(\text{Ph})\text{CH}_2\text{CH}_2\text{CH}=\text{CH}_2$) from $[\text{Ir}(\text{Cl})(\text{cod})]_2$.

Our interest in the cod complexes of iridium(I) stems from the ability of these complexes to undergo oxidative addition reactions with CH_3I . The catalytic production of acetic acid from methanol using both rhodium(I) and iridium(I) complexes involve the key step of oxidative addition, which is then followed by methyl migration, reductive elimination and finally substitution to produce acetic acid and the original metal complex. Research has shown

that the iridium complex¹⁵ is by far the superior catalyst (faster reactions, milder experimental condition, increased robustness and selectivity) and in order to understand the chemistry of these complexes, different ligands are bonded to the metal centre to improve reactivity and selectivity.^{16,17}

Our research has shown that the methyl migration step (or CO insertion) spontaneously follows the oxidative addition reaction.¹⁸ These consecutive or sometimes simultaneous reactions (depending on the rate of the two steps) complicate the kinetics and overall mechanism, which include different isomers and equilibria, solvent assisted reaction pathways and non-zero intercepts. High-pressure studies in these cases involve a complete ligand variation at different temperatures to determine the activation volumes of these reactions. The absence of the carbonyl ligand from the cod complexes simplify the overall reaction since no CO insertion can take place, one isomer is normally produced due to the steric influence of the cod on the final $[\text{Ir}(\text{cod})(\text{LL}')(\text{CH}_3)\text{I}]$ complex and simplified mechanisms with zero intercept are normally obtained. This allows for the isolated influence of the different ligands on the oxidative addition step, as well as simplified high-pressure studies.

$[\text{Ir}(\text{cod})(\text{sacac})]$ (sacac = thioacetyl acetonato) was synthesized in this study to determine the rate and the mechanism of the oxidative addition step in different solvents, as well as to determine the intrinsic activation volume for this complex. Experimental results are complimented by theoretical density functional theory (DFT) results on the geometries and energies of the reactants, transition state and possible products of the $[\text{Ir}(\text{sacac})(\text{cod})]$ and CH_3I reaction.

2. Experimental

2.1. General considerations

Unless otherwise stated, all chemicals were reagent grade and used without further purification and all preparations carried out in air. Sacac was prepared with slight variations of previously reported methods. IR spectra were recorded with a Hitachi 270-50 spectrophotometer while the NMR spectra (TMS as internal standard) were obtained at 293 K on a Bruker 600 MHz spectrometer. The methyl iodide was stabilized by silver foil to prevent decomposition and used in a well-ventilated fume cupboard. The CHN analysis was

performed on a LECO Truspec micro-analyser while the iridium analysis was performed on a Shimadzu ICPS-7510 ICP-OES sequential plasma spectrometer. MALDI-TOF spectra were collected by a Bruker Microflex LRF20 in the positive mode with the minimum laser power required to observe signals.

The UV/visible spectra and kinetic runs were performed on a Hitachi 150-20 UV/visible spectrophotometer in a thermostatically controlled holder (0.1°C), which has a capacity of 6 cells. The solvents used for the kinetic runs were all purified and dried using prescribed methods.¹⁹ All the complexes were tested for stability in the different solvents prior to the kinetic runs. High-pressure kinetics was performed on a GBC (model 916) UV/VIS spectrophotometer equipped with a temperature-controlled high-pressure cell. Activation volumes were calculated from kinetic runs at elevated pressure using the mathematical relationship $\ln k = -(\Delta V^\ddagger/RT)p$. Typical experimental conditions were $[M(\text{cod})(\text{LL}')]$ = 5.0×10^{-4} M, and $[\text{CH}_3\text{I}]$ varied between 0.075 and 0.75 M, which ensured good pseudo-first-order kinetics. The observed first-order rate constants (k_{obs}) were calculated for at least two half-lives from the above plots using the equation $A_t = A_\infty + (A_0 - A_\infty)e^{(-k_{\text{obs}}*t)}$ with A_0, A_t and A_∞ the absorbances at time 0, t and infinity respectively, using a non-linear least squares program.²⁰

2.2. Synthesis

Thioacetyl acetonato ligand (sacac) was synthesized by two different methods as proposed by Mayer.²¹

2.2.1. Acid catalysis

Dry H_2S gas was bubbled through a solution containing 15 mL acetyl acetone in 225 mL acetonitrile at -44°C for 90 min. Subsequently dry HCl (from NH_4Cl and H_2SO_4 and bubbled through dry H_2SO_4) was bubbled through the mixture for 120 min during which time the colour of the solution changed from colourless to light yellow and then dry H_2S gas for another 180 min at -40° . The mixture was then added to 370 mL ice water, 225 mL n-pentane and 75 mL diethyl ether while continuously stirring the mixture. The aqueous layer was extracted twice with 200 mL n-pentane/ether mixture (3:1). The organic layer was

washed with two 50 mL portions of water (pH ~5.5) and dried over anhydrous Na₂SO₄. The solution was filtered and concentrated with reduced pressure. The red-brown oil was fractionally distilled under reduced pressure (5 mmHg) to yield bright yellow oil. Yield: 24%.

2.2.2. Base catalysis

Acetyl acetone (50 mL, 0.5 mol) and morpholine (4.3 g, 0.05 mol) was mixed in a long cylindrical container. Small H₂S gas bubbles were introduced for 180 min at the bottom of the container with the aid of a long glass pipe and a sinter glass frit to ensure effective gas to solution mass transfer. The un-reacted H₂S gas was removed by leading the spent gas through a concentrated NaOH solution. The container was sealed and left at room temperature overnight. The mixture was subsequently washed with 100 mL of petroleum ether (b.p. 80 -100°C) and then with 3M HCl. The crude product was dried over anhydrous Na₂SO₄ and concentrated with reduced pressure. The final gold-yellow product was obtained by fractional distillation at 40°C and 5 mmHg. Yield: 71%.

2.2.3. (η^4 -1,5-Cyclooctadiene)(thioacetylacetonato)iridium(I), [Ir(cod)(sacac)]

0.1 g [IrCl(cod)]₂ was dissolved in a minimum (~ 10 mL) of dimethylformamide (DMF). 0.35 mL thioacetyl acetone dissolved in 3 mL DMF, was added to the first solution while stirring. Water was added drop wise to the reaction mixture, which afforded the precipitation of a yellow product. The precipitate was separated from the mother solution with centrifugation and decantation. The product was subsequently dissolved in a minimum of acetone and re-crystallized with the drop wise addition of water and separated from the mother solution with centrifugation and decantation. The yellow product was washed with water, centrifuged and dried over P₂O₅.

Yield: 62 %. IR: ν (Ir-S), 360, ν (C-S), 663, 738, ν (C-H), 2920, ν (C=C), 1230 cm⁻¹. Elemental analysis (calculated values in brackets): C, 37.10 (37.58), H, 4.49 (4.60), S, 6.93 (7.72), Ir, 46.0 (46.26)%.; ¹H NMR (600 MHz, CDCl₃): δ 1.79-1.86 (m, 4H), 2.09 (s, 3H), 2.15-2.25 (m, 4H), 2.35 (s, 3H), 3.81 (dd, 2H), 4.35 (dd, 2H), 6.57 (s, 1H); ¹³C NMR (600 MHz, CDCl₃): δ 187.3, 179.9, 119.9, 74.1, 53.4, 33.1, 31.9, 30.2, 29.3 ppm. m/z(M-H)⁺: 413.05(29.81), 414.06(5.53), 415.03(48.83), 416.05(11.36), 417.04(3.81) 418.09(4.61%)

2.2.4. (η^4 -1,5-Cyclooctadiene)(iodo)(methyl)(thioacetylacetonato)iridium(III),
 [Ir(cod)(sacac)(CH₃)I]

An excess of CH₃I and [Ir(cod)(sacac)] (0.2 g, 0.47 mmol) was mixed in 2 mL acetone. The solution was sealed for 60 min. The seal was removed and the solution was concentrated in a vacuum desiccator. The concentrated solution was kept at -10 °C and orange needles, suitable for an X-ray crystal structure determination was obtained from the solution.²²

IR: ν (Ir-S), 360, ν (C-S), 663, 738, ν (C-H), 2920, ν (C=C), 1230 cm⁻¹. Elemental analysis (calculated values in brackets): C, 30.65 (30.16), O, 5.14 (5.85), H, 4.04 (3.98), S, 2.66 (2.87), I 22.10, (22.76), Ir, 35.5 (34.48) %.; ¹H NMR (600 MHz, CDCl₃): δ 1.87-1.91 (m, 1H), 1.92 (s, 3H), 2.10 (s, 3H), 2.23-2.30 (m, 1H), 2.23-2.30 (m, 1H), 2.36 (s, 3H), 2.52-2.66 (m, 1H), 2.52-2.66 (m, 1H) 2.52-2.66 (m, 1H) 2.98-3.05 (m,1H), 3.20-3.29 (m, 1H), 3.98-4.02(m, 1H), 4.68-4.73 (m, 1H), 4.91-4.97 (m, 1H), 5.60-5.64 (m, 1H), 6.37 (s, 1H); ¹³C NMR (600 MHz, CDCl₃): δ 187.6, 179.2, 118.5, 95.4, 94.6, 72.0, 71.1, 34.9, 31.7, 31.3, 30.4, 30.3, 26.0, 11.1 ppm. m/z(M-I)⁺: 429.10(30.15), 430.10(4.76), 431.10(52.91), 432.11(8.46), 433.10(3.17) 434.10(0.52%)

2.3. Kinetics

The UV/visible spectrum of the oxidative addition reaction between [Ir(cod)(sacac)] and methyl iodide in acetone showed one reaction with the formation of three isosbestic points (see **Figure 1**). The formation of isosbestic points were also observed in different solvents as well as for the other complexes. A summary of the observed isosbestic points for the different complexes is given in **Table 1**. Initial variations of methyl iodide concentrations indicated a linear relationship with intercept close to zero as illustrated by the oxidative addition of CH₃I to Ir(cod)(sacac)] in chloroform in **Figure 2**.

Table 1. Summary of the kinetic data and activation parameters for the oxidative addition reactions between [Ir(cod)(sacac)] and CH₃I in different solvents

Solvent	Isosbestic points (nm)	ϵ_0	q_p (10 ⁶)	k_1 (10 ³) (M ⁻¹ s ⁻¹)	k_{-1} (10 ⁴) (s ⁻¹)	ΔH^\ddagger (kJ mol ⁻¹)	ΔS^\ddagger (J K ⁻¹ mol ⁻¹)	ΔV^\ddagger (cm ³ mol ⁻¹)
Chloroform	363;402;446	4.64	16.7	2.5(2)	-	61(10)	-88(35)	+10.2(9)
Chlorobenzene	364;405;455	5.44	10.2	1.78(5)	9(2)	54(6)	-115(20)	-
Dichloromethane	361;401;440	8.54	11.5	4.5(4)	-	45(7)	-139(23)	-3.7(2)
Acetone	358;400;450	19.7	6.4	3.4(2)	-	25.5	-207(1)	-5.9(4)
Acetonitrile	354;408;437	36.1	1.5	5.2(3)	-	35(4)	-170(12)	-19(1)

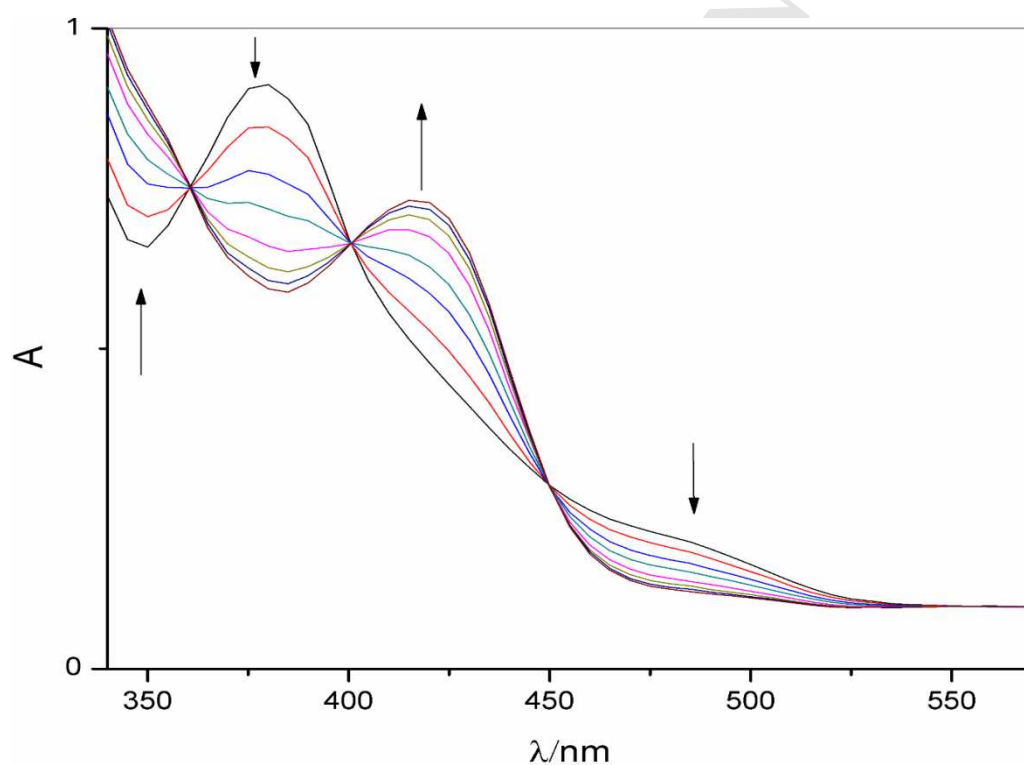


Figure 1. Spectrum change with the addition of CH₃I to [Ir(cod)(sacac)] in acetone at 298 K and 10 min. intervals, [CH₃I] = 0.75 M.

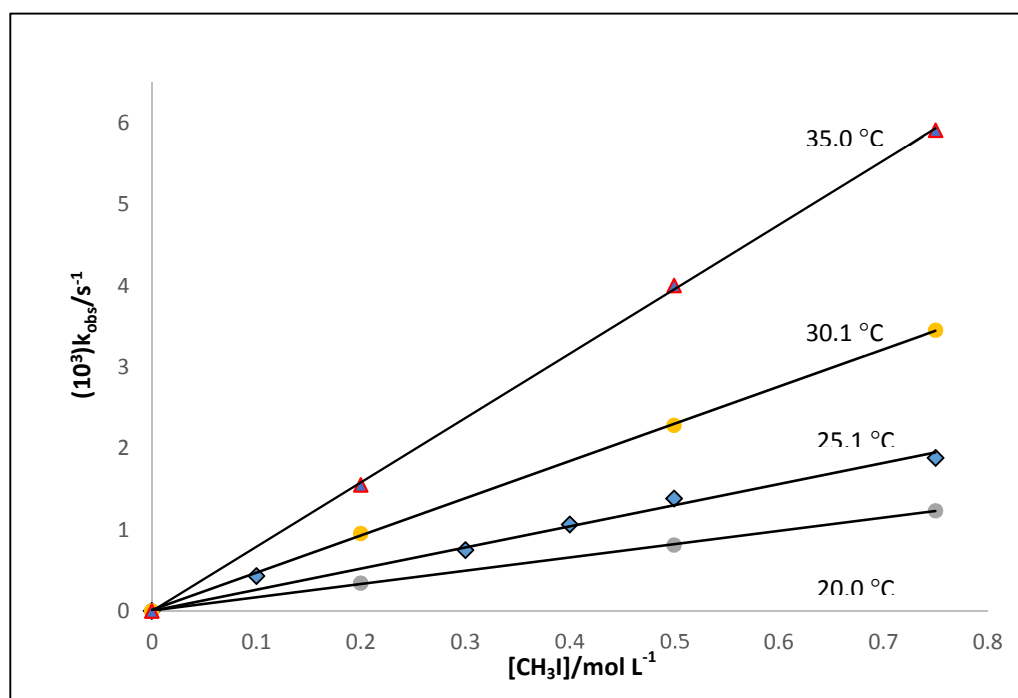
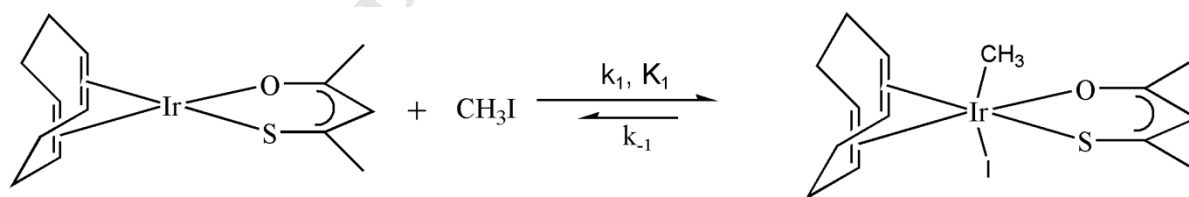


Figure 2. k_{obs} vs $[\text{CH}_3\text{I}]$ in chloroform at different temperatures, $[\text{Ir}(\text{cod})(\text{sacac})] = 5.0 \times 10^{-4} \text{ mol L}^{-1}$

These results led to a very simple reaction mechanism **Scheme 1**.



Scheme 1: Oxidative addition between $[\text{Ir}(\text{sacac})(\text{cod})]$ and CH_3I

The rate law for this potential reversible reaction is given by **Equation 1**

$$R = k_1[\text{Ir}(\text{cod})(\text{sacac})][\text{CH}_3\text{I}] - k_{-1}[\text{Ir}(\text{cod})(\text{sacac})(\text{CH}_3)\text{I}] \quad \dots 1$$

The observed rate constant, after integration and using pseudo-first-order conditions are given by **Equation 2**

$$k_{\text{obs}} = k_1[\text{CH}_3\text{I}] + k_{-1}$$

...2

A summary of the calculated rate constants as well as activation parameters are given in **Table 1**. These values indicated that the k_{-1} values for the different complexes, with the exception of the reaction in chlorobenzene are all zero within experimental error. The high-pressure kinetics between $[\text{Ir}(\text{cod})(\text{sacac})(\text{cod})]$ and CH_3I were performed in four different solvents, namely chloroform, dichloromethane, acetone and acetonitrile in order to determine the intrinsic volume of activation for this reaction. The results are presented in **Figure 3**.

Table 2. Summary of the kinetic data for the oxidative addition reactions between different $[\text{Ir}(\text{cod})(\text{LL})]$ and CH_3I in different solvents and bidentate ligands with different ring sizes at 25 °C.

Complex	Donor atoms	Ring size	k_1 ($\times 10^2$) ($\text{M}^{-1} \text{s}^{-1}$)	Solvent	Ref
$[\text{Ir}(\text{acac})(\text{cod})]$	O,O	6	1.69(2)	Acetone	23
$[\text{Ir}(\text{tfaa})(\text{cod})]$	O,O	6	0.133(2)	Acetone	23
$[\text{Ir}(\text{cod})(\text{sacac})]$	S,O	6	0.52(3)	Acetonitrile	This study
	S,O	6	0.34(2)	Acetone	This study
$[\text{Ir}(\text{cod})(\text{AnMetha})]$	S,O	5	2.69(6)	Nitromethane	24
$[\text{Ir}(\text{cod})(\text{hpt})]$	S,O	5	2.2(2)	Nitromethane	24
$[\text{Ir}(\text{cod})(\text{bpt-NH})]$	N,N	6	1.44(7)	Dichloromethane	25
$[\text{Ir}(\text{cod})(\text{AnMetha})]$	S,O	5	0.943(10)	Acetone	24
$[\text{Ir}(\text{cod})(\text{hpt})]$	S,O	5	0.693(17)	Acetone	24
$[\text{Ir}(\text{cod})(\text{bpt})]$	N,N	5	0.35(1)	Acetone	25
$[\text{Ir}(\text{cod})(\text{bpt-NH})]$	N,N	6	0.0919(4)	Benzene	25

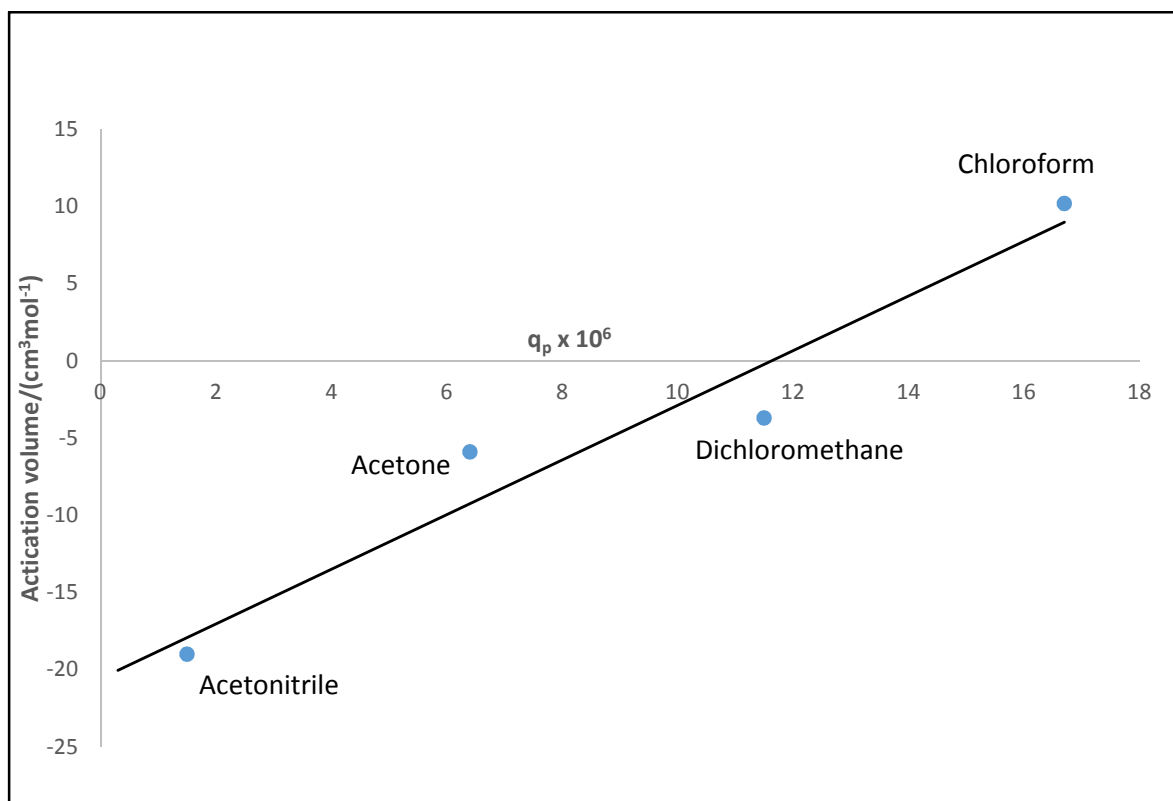


Figure 3. Plot of the q_p value of the different solvents vs volume of activation for [Ir(cod)(sacac)]

2.4. DFT study

The DFT calculations were carried out with the ADF (Amsterdam Density Functional) 2013 program system²⁶ employing the PW91 (Perdew-Wang 1991)²⁷ GGA (Generalized Gradient Approximation) functional, a Slater-type TZP (triple- ζ plus polarization) basis set, a fine mesh for numerical integration, and full geometry optimizations with tight convergence criteria. All structures were calculated as singlet states ($S = 0$) and the geometry optimizations were all symmetry-unconstrained. All transition states were confirmed with frequency analyses and exhibited a single imaginary frequency. Zero-point energy and thermal corrections (vibrational, rotational and translational) were made to the electronic energies in the calculation of the thermodynamic parameters. Enthalpies (H) and Gibbs free energies (G) were calculated from:

$$U = E_{el} + E_{ZPE} \quad \dots 3$$

$$H = U + RT \text{ (for gas phase); or } H = U \text{ (in solution)} \quad \dots 4$$

$$G = H - TS \quad \dots 5$$

where U = the total energy, E_{el} = total electronic energy, and E_{IE} = internal energy (sum of vibrational, rotational, translational energies including the zero-point energy correction); R = ideal gas constant, T = temperature and S = entropy. The entropy (S) was calculated from the temperature dependent partition function in ADF at 298.15 K. The calculated results assume an ideal gas unless where indicated that solvent effects were taken into account. Where indicated, the COSMO (Conductor like Screening Model) model of solvation²⁸ was used as implemented in ADF. The type of cavity used was Esurf²⁹ and the solvents used were acetone and acetonitrile ($\epsilon_0 = 20.7$ and 37.5 respectively). Scalar relativistic effects were used with the ZORA³⁰ (Zero Order Regular Approximation) formalism.

3. Discussion of results

3.1. Synthesis

[Ir(cod)(sacac)] as well as [Ir(sacac)(cod)](CH₃)(I) were successfully isolated and characterised with ¹H and ¹³C NMR, IR metal analysis, as well as with infrared spectroscopy.²⁶ The protons (eight) of the four methylene groups of cyclobutadiene in the starting material are observed as two broad peaks at δ 1.79-1.86 and δ 2.15-2.25 ppm in the ¹H NMR spectrum. The same protons in the oxidative addition product are assigned as four broad multiplets at δ 1.87-1.91, 2.23-2.30, 2.52-2.66 and 2.98-3.29 ppm due to the splitting of these protons (axial and equatorial position) as a result to the different chemical environment induced by the methyl and the iodide in the product. The axial protons inside the ring are more deshielded than those outside the ring and therefore appear downfield compared to the equatorial protons. The double bond protons (four) of the cyclobutadiene appear as two peaks at δ 3.81 and 4.35 ppm in the starting material which are then split into four multiplets at δ 3.98-4.02, 4.68-4.73, 4.91-4.97 and 5.60-5.64 ppm in the oxidative addition product due to different chemical environment above and below the plane.

The proton at the alpha position (methine) in the sacac ligand, adjacent to the oxygen and sulphur display a distinct downfield shift due to the conjugation in the ring structure. The

proton in the starting material and product appears as singlets at δ 6.57 and 6.37 ppm respectively and their downfield shift is also attributed to the electron withdrawing effects imposed by the sacac moiety. The two methyl groups in [Ir(cod)(sacac)] is assigned as singlets at δ 2.09 and 2.35 ppm while an additional methyl peak at δ 1.92 ppm is observed in [Ir(sacac)(cod)](CH₃)(I), confirming the coordination of the methyl iodide to the iridium centre. The ¹³C NMR showed the presence of fourteen carbons in the product (as expected due to chemical difference above and below the plane) while the APT experiment showed eight carbons in the negative mode (even number of protons) and six carbons in the positive mode (odd or uneven number of protons) for the methylene groups and quaternary carbons respectively.

The cod protons in the region of 4.35 to 1.5 ppm compare favourably with the 3.80 to 1.80 ppm for [Ir(triazolato)(cod)] (triazolato = 3,5-bis(pyridine-2-yl)-1,2,4 triazolate (bpt-NH) and 4-amino-3,5-bis(pyridine-2-yl)-1,2,4 triazolate (bpt))³¹ and 4.40 to 1.70 ppm for [Ir(S,O)(cod)] (S,O = N-methyl-p-methoxybenzathiohydroxaminato and 1-hydroxi-2-pyridinato ligands)²⁴

3.2 Kinetics

The formation of isosbestic points with the addition of methyl iodide to [Ir(sacac)(cod)] solutions in different solvents clearly indicate the formation of only one product, namely the Ir(III) alkyl product^{26,32}



The kinetic results of the oxidative addition of CH₃I to [Ir(cod)(sacac)] for all the solvent studied showed simple second order kinetics with almost no reversible reaction as indicated by the zero intercept (within experimental error). Surprisingly, the rate of oxidative addition with a solvent variation showed little or no change (factor 2 difference) with a large difference in polarity for the selected solvents (q_p between 1.5×10^{-6} and 16.7×10^{-6}). An increase of a factor 9 and 4 was observed for the [Ir(sacac)(cod)] complexes while an increase of 20 to 40 was observed for the [Rh(sacac)(CO)(PPh₃)]²⁵ complex with a solvent variation. A comparison of the rate of oxidative addition for the different iridium cod complexes in **Table 3** show a relatively small variation in rate constant with a variation

of bidentate ligands, ring size and solvent and varies between $9.19(4) \times 10^{-4}$ and $2.69(6) \times 10^{-2} \text{ M}^{-1} \text{ s}^{-1}$ (factor 30) for $[\text{Ir}(\text{cod})(\text{bpt-NH})]$ and $[\text{Ir}(\text{cod})(\text{AnMetha})]$ respectively.

Table 3. PW91/TZP DFT calculated electronic (E) and Gibbs free (G) energies (kJ mol^{-1}) of the possible transition states (TS) and possible products of the $[\text{Ir}(\text{sacac})(\text{cod})] + \text{CH}_3\text{I}$ oxidative addition reaction, relative to the energy of the reactants as 0.

	Gas phase		Acetone		Acetonitrile	
	ΔE	$\Delta G^{298\text{K}}$	ΔE	$\Delta G^{298\text{K}}$	ΔE	$\Delta G^{298\text{K}}$
$\text{Ir(I)} + \text{CH}_3\text{I}$	0.0	0.0	0.0	0.0	0.0	0.0
TS <i>cis</i> 1	147.8	189.8	158.6	201.3	158.7	201.5
TS <i>cis</i> 2	147.7	192.0	157.9	205.4	157.9	205.5
TS <i>trans</i>	35.8	85.2	30.3	81.1 (87 exp)	29.9	80.7 (86 exp)
$\text{Ir(III)-alkyl cis 1}$	-33.8	22.9	-38.8	21.3	-39.4	20.7
$\text{Ir(III)-alkyl cis 2}$	-8.9	44.1	-7.2	45.8	-7.2	45.8
$\text{Ir(III)-alkyl cis 3}$	-26.0	36.8	-31.0	29.7	-31.4	29.3
$\text{Ir(III)-alkyl cis 4}$	-11.9	38.7	-11.5	43.4	-11.7	43.2
$\text{Ir(III)-alkyl trans}$	-40.5	19.6	-47.4	13.7	-48.1	13.0

The negative activation entropy values for all the reactions are indicative of associative activation during the transition state. The high-pressure study, which was performed on $[\text{Rh}(\text{sacac})(\text{cod})]$ complex with a variation of solvents is clearly illustrated in Figure 3. The linear relationship between the experimentally obtained activation volume and q_p values are indicative for reactions that obey the Kirkwood equation^{33,34}, which predicts a linear relationship between activation volumes and solvent polarity ($\Delta V_{\text{exp}}^{\ddagger} = \Delta V_{\text{intr}}^{\ddagger} + \Delta V_{\text{solv}}^{\ddagger}$ (or $N\Delta u^2/r^3 q_p$)). An extrapolation of this graph yields an intrinsic volume of activation, $\Delta V_{\text{intr}}^{\ddagger}$, of $-21(3) \text{ cm}^3 \text{ mol}^{-1}$. This result indicates that the same transition state exists between $[\text{Ir}(\text{sacac})(\text{cod})]$ and CH_3I for the solvents used in this study and this value corresponds favourably with the -17 and $-14.7 \text{ cm}^3 \text{ mol}^{-1}$ obtained for $[\text{IrCl}(\text{CO})(\text{PPh}_3)_2]$ ³⁵ and $[\text{Rh}(\text{sacac})(\text{cod})]$.²⁵ The negative value for the intrinsic volume of activation is indicative of associative activation during the transition state. The largest negative activation volumes

were obtained for the more polar solvents, which suggest charge separation (formation of a linear transition state) during the oxidative addition of the CH_3I to the metal complex.

3.3 DFT study

The oxidative addition reaction of CH_3I to $[\text{Ir}(\text{cod})(\text{sacac})]$ may theoretically lead to five possible reaction products: one *trans* and four *cis* $[\text{Ir}(\text{cod})(\text{sacac})(\text{CH}_3)(\text{I})]$ -alkyl products. The density functional theory (DFT) calculated optimized geometry and relative energies of the five possible $[\text{Ir}(\text{cod})(\text{sacac})(\text{CH}_3)(\text{I})]$ -alkyl products are presented in **Figure 4** and **Table 3** respectively. The gas phase DFT results, in acetone or acetonitrile as solvent, all show that *trans* $[\text{Ir}(\text{cod})(\text{sacac})(\text{CH}_3)(\text{I})]$ -alkyl has the lowest energy. This result is in agreement with the experimental crystal structure obtained for $[\text{Ir}(\text{cod})(\text{sacac})(\text{CH}_3)(\text{I})]$ with methyl and iodide in the *trans* position.²⁶ Although the energy of $[\text{Ir}(\text{cod})(\text{sacac})(\text{CH}_3)(\text{I})]$ -alkyl *cis* 4 is within 10 kJ mol^{-1} of that of *trans* $[\text{Ir}(\text{cod})(\text{sacac})(\text{CH}_3)(\text{I})]$ -alkyl, the energy needed for *cis* addition to occur is too high (**Table 3**). Therefore *trans* addition is favoured and *trans* $[\text{Ir}(\text{cod})(\text{sacac})(\text{CH}_3)(\text{I})]$ -alkyl is the only expected reaction product, in agreement with experimental observation.²⁶

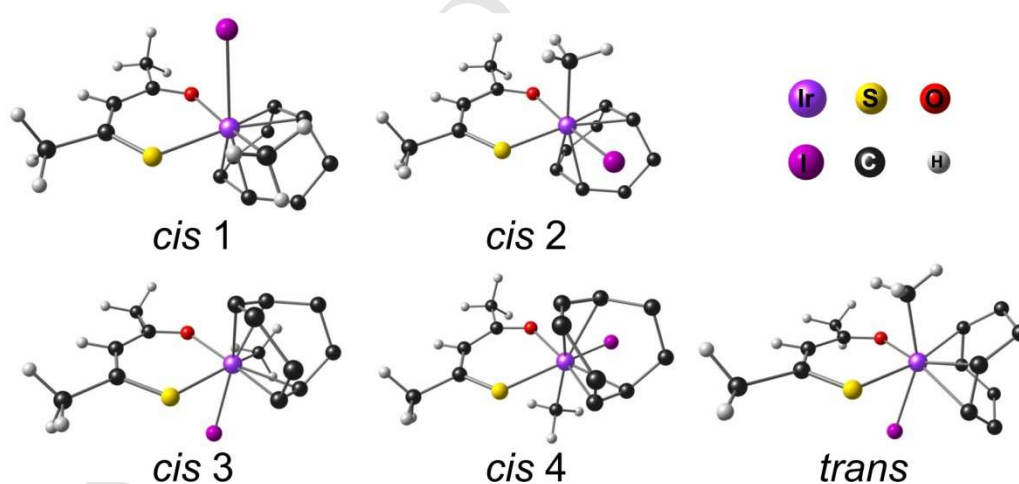


Figure 4. DFT (PW91/TZP gas phase) optimized geometries of the five possible reaction products of the $[\text{Ir}(\text{cod})(\text{sacac})] + \text{CH}_3\text{I}$ reaction. The H-atoms on the cod ligand are omitted for clarity.

During the oxidative addition step, the CH_3I can approach $[\text{Ir}(\text{cod})(\text{sacac})]$ with the $\text{CH}_3\text{-I}$ bond approximately perpendicular (*trans* addition) or parallel (*cis* addition) to the plane

through the sacac-backbone, Ir and cod. During *cis* addition, the CH₃I can be orientated with the CH₃ group on the side of the oxygen of sacac (*cis* 1 addition) or on the side nearer to sulphur of sacac (*cis* 2 addition). In **Figure 5** the optimized structures of the *trans* and two possible *cis* transition states (TS) of CH₃I to [Ir(cod)(sacac)] are given with the activation energies tabulated in **Table 3**. For all three possible TS the vibrational analysis showed only one imaginary frequency (279i, 295i and 278i for TS *cis* 1, TS *cis* 2 and TS *trans* respectively, obtained for PW91/TZP gas phase), which characterized unambiguously the stationary points as true TS structures. The *trans* addition is energetically favoured by a large margin of energy. The DFT calculated activation free energy given in **Table 3** are in good agreement with the experimental activation free energy obtained, 86 – 88 kJ mol⁻¹, depending on the reaction solvent.

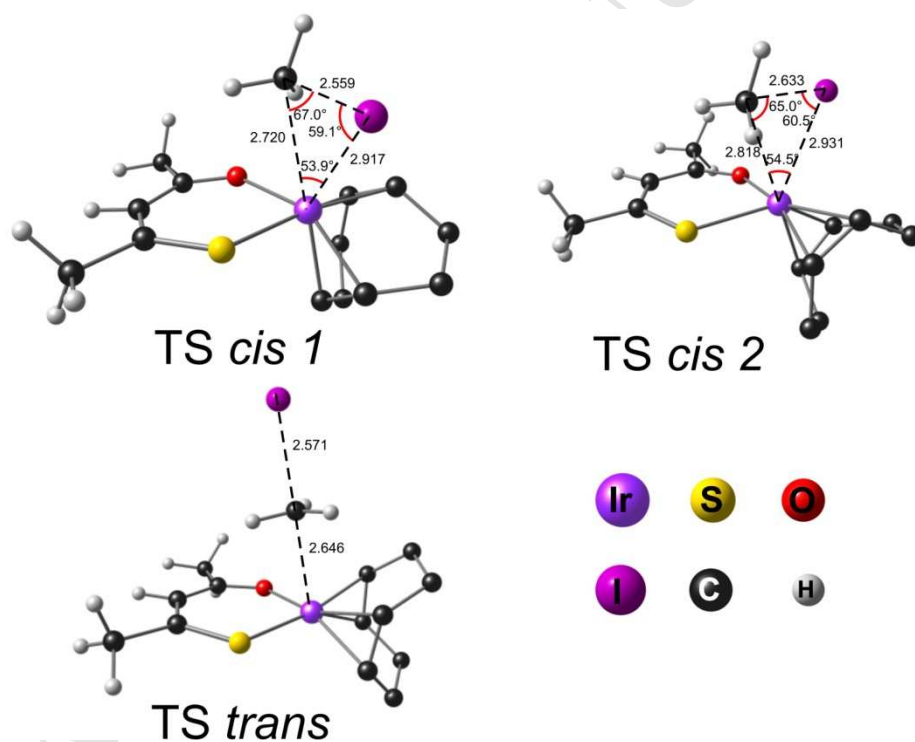


Figure 5. DFT (PW91/TZP gas phase) optimized geometries of the three possible transition states for the [Ir(cod)(sacac)] + CH₃I reaction. Selected bond lengths (Å) and angles (°) are indicated. The H-atoms on the cod ligand are omitted for clarity.

The HOMO of the *trans* transition state geometry in **Figure 6** shows that *trans* addition begins with the attack of two non-bonding electrons of the Ir d₂₂ at the empty orbital of p_z

character on the CH₃ group of CH₃I. A cationic five-coordinated trigonal pyramidal intermediate is formed and the oxidation state of iridium changes from Ir(I) to Ir(III). This is followed by the fast barrier less addition of a I⁻ ion to the vacant 2e⁻ site on Ir(III) leading to an increase by 2e⁻ in the electron count (I⁻ is a 2e⁻ reagent) from the 16e⁻ complex to an 18e⁻ complex.

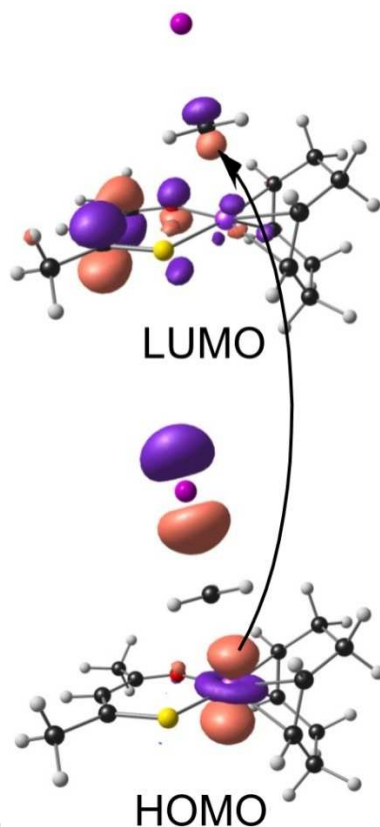


Figure 6. DFT calculated HOMO and LUMO of the optimized geometry of the linear transition state of the $[[\text{Ir}(\text{cod})(\text{sacac})] + \text{CH}_3\text{I}]$ reaction oxidative addition reaction. The attack of two non-bonding electrons of the Ir d_{z^2} of the HOMO at the empty LUMO of p_z character on the CH₃ group of CH₃I is shown by an arrow. The MO plots use a contour of 60 e/nm³. Colour code of atoms (online version): Ir (purple), I (magenta), C (black), N (yellow), O (red), H (white).

4. Conclusion

Experimental and theoretical DFT results on the oxidative addition reaction of CH₃I to $[\text{Ir}(\text{cod})(\text{sacac})]$ both showed that the reaction occurs in one step resulting in *trans* $[\text{Ir}(\text{cod})(\text{sacac})(\text{CH}_3)(\text{I})]$ -alkyl. A DFT analysis of the oxidative addition reaction shows that the *trans* addition involves the attack of two non-bonding d_{z^2} -electrons on Ir at the empty p_z

orbital of the CH_3 group of CH_3I with the formation of a cationic five-coordinated trigonal pyramidal intermediate, followed by the fast addition of an I^- ion to the vacant $2e^-$ site on Ir(III) . The experimental negative activation entropy obtained, supports the associative activation while the difference in volume of activation points to charge separation during the transition state.

Acknowledgements

This work has received support from the Norwegian Supercomputing Program (NOTUR) through a grant of computer time (Grant No. NN4654K) (JC), the South African National Research Foundation and the Central Research Fund of the University of the Free State, Bloemfontein, South Africa.

Supporting Information

The optimized coordinates of the DFT calculations.

References

1. R. H. Crabtree, *Accounts Chem. Res.*, 12 (1979) 331-337.
2. J. Cipot, R. McDonald, M. Stradiotto, *Chem. Commun.*, (2005) 4932-4934.
3. L. D. Vazquez-Serrano, B. T. Owens, J. M. Buriak, *Inorg. Chim. Acta.*, 359 (2006) 2786-2797.
4. T. Saiki, Y. Nishio, T. Ishiyama, N. Miyaura, *Organometallics*, 25 (2006) 6068-6073.
5. J. Takagi, K. Sato, J.F. Hartwig, T. Ishiyama, N. Miyawa, *Tetrahedron Lett.*, 43 (2002) 5649-5651.
6. I. Matsuda, Y. Hasegawa, T. Makino, K. Itoh, *Tetrahedron Lett.*, 41 (2000) 1405-1408.
7. L.A. Ora, J.A. Cabeza, C. Cativiela, M.D. Diaz de Villegas, E. Meléndez, *J. Chem. Soc. Chem. Comm. Commun.*, (1983) 1383-1384.
8. J.A. Cabeza, C. Cativiela, M.D. Diaz de Villegas, L.A. Ora, *J. Chem. Soc. Perk. T. 1*, (1988) 1881-1884.
9. A. Lightfoot, P. Schnider, A. Pfaltz, *Angew. Chem. Int. Edit.*, 37 (1998) 2897-2899.
10. M.A. Esteruelas, A.M. Lopez, L.A. Oro, A. Pérez, M. Shulz, H. Werner, *Organometallics*, 12 (1993) 1823-1830.
11. K.R. Lee, M.-S. Eum, C.S. Chin, S.C. Lee, I.J. Kim, Y.S. Kim, Y. Kim, S.-J. Kim, N.H. Hur, *Dalton Trans.*, (2009) 3650-3652.
12. C.S. Chin, W.-T. Chang, S. Yang and, K.-S. Joo, *Bull. Kor. Chem. Soc.*, 18 (1997) 324-327.
13. R.B. Bedford, P.A. Chaloner, P.B. Hitchcock, *Acta Crystallogr. C*, 50 (1994) 354-356.
14. Y.W. Park, D.W. Meek, *Bull. Kor. Chem. Soc.*, 16 (1995) 524-528.
15. T.W. Dekleva, D. Foster, *Adv. Catal.*, 34 (1986) 81-130.
16. A. Haynes, P.M. Maitlis, G.E. Morris, G.J. Sunley, H. Adams, P.W. Badger, C.M. Bowers, D.B. Cook, P.I.P. Elliot, T. Ghaffar, H. Green, T.R. Griffin, M. Payne, J.-M. Pearson, M.J. Taylor, P.W. Vickers, R. J. Watt, *J. Am. Chem. Soc.*, 126 (2004) 2847-2861.
17. P.M. Maitlis, A. Hayes, G.J. Sunley, M.J. Howard, *J. Chem. Soc., Dalton trans.*, (1996) 2187-2196.

18. J.G. Leipoldt, E.C. Steynberg, R. van Eldik, *Inorg. Chem.*, 26 (1987) 3068-3070; J.A. Venter, J.G. Leipoldt, R. Van Eldik, *Inorg.Chem.*, 30 (1991) 2207-2209; M.M. Conradie, J.J.C. Erasmus, J. Conradie, *Polyhedron*, 30 (2011) 2345-2353; N.F. Stuurman, J. Conradie, *J. Organomet. Chem.*, 694 (2009) 259-268; M.M. Conradie, J.Conradie, *Inorg. Chim. Acta.*, 361 (2008) 2285-2295; J. Conradie, J.C. Swarts, *Organometallics*, 28 (2009) 1018-1026; M.M. Conradie, J. Conradie, *Inorg. Chim. Acta.*, 362 (2009) 519-530.
19. D.D. Perrin, W.L.F. Armarego, *Purification of Laboratory Chemicals*, 3rdEd., Pergamon Press, Oxford, (1988).
20. Scientist, Version 2, MicroMath Scientific Software, Saint Louis, Mo (2004).
21. R. Mayer, G. Hiller, M. Nitzschke, *Angew. Chem.*, 2 (1963) 370-373.
22. Y.M. Terblans, S.S. Basson, W. Purcell, G.J. Lamprecht, *Acta Crystallogr. C*, 51 (1995) 1748-1750.
23. S.S. Basson, J.G. Leipoldt, W. Purcell, J.B. Schoeman, *Inorg. Chim. Acta.*, 173, (1990,) 155-158.
24. M. Theron, E. Grobbelaar, W. Purcell, S.S. Basson, *Inorg. Chim. Acta.*, 358 (2005) 2457-2463.
25. J.G. Leipoldt, S.S. Basson, L.J. Botha, *Inorg. Chim. Acta.*, 168 (1990) 215-220.
26. ADF2013, SCM, Theoretical Chemistry, Vrije Universiteit, Amsterdam, The Netherlands, The ADF program system uses methods described in: G. teVelde, F. M. Bickelhaupt, E. J. Baerends, C. F. Guerra, S. J. A. van Gisbergen, J. G. Snijders, T. Ziegler, *J. Comput. Chem.*, 22 (2001) 931-967.
27. J.P. Perdew, J.A. Chevary, S.H. Vosko, K.A. Jackson, M.R. Pederson, D.J. Singh, C. Fiolhais, *Phys. Rev. B* 46, 46 (1992) 6671. Erratum: J.P. Perdew, J.A. Chevary, S.H. Vosko, K.A. Jackson, M.R. Pederson, D.J. Singh, C. Fiolhais, *Phys. Rev. B*, 48 (1993) 4978.
28. A. Klamt, G. Schüürmann, *J. Chem. Soc. Perkin T. 2* (1993) 799-805; A. Klamt, *J. Phys. Chem.*, 99 (1995) 2224-2235; A. Klamt, V.J.Jones, *Chem. Phys.*, 105 (1996) 9972-9981.
29. J.L. Pascual-Ahuir, E. Silla, I. Tuñon, *J. Comput. Chem.*, 15 (1994) 1127-1138.

30. E. van Lenthe, A. Ehlers, E.J. Baerends, *J. Chem. Phys.*, 110 (1999) 8943-8953; E. van Lenthe, E.J. Baerends, J.G. Snijders, *J. Chem. Phys.*, 99 (1993) 4597-4610; E. van Lenthe, E.J. Baerends, J.G. Snijders, *J. Chem. Phys.*, 101 (1994) 9783-9792; E. van Lenthe, J.G. Snijders, E.J. Baerends, *J. Chem. Phys.*, 105 (1996) 6505-6516; E. van Lenthe, R. van Leeuwen, E.J. Baerends, J.G. Snijders, *Int. J. Quantum Chem.*, 57 (1996) 281-293.
31. A.J. Muller, J. Conradie, W. Purcell, S.S. Basson, J.A. Venter, *S. Afr. J. Chem.*, 63 (2010) 11-19. <http://www.journals.co.za/sajchem/>
32. S.S. Basson, J.G. Leipoldt, W. Purcell, J.B. Schoeman, *Acta Crystallogr. C*, 45 (1989) 2000-2001.
33. J.G. Kirkwood, *J. Chem. Phys.*, 2 (1934) 351.
34. N. Isaacs, *Liquid Phase High Pressure Chemistry*, Wiley, Chichester (1981).
35. H. Steiger, H. Helm, *J. Phys. Chem.*, 77 (1973) 290.

Research highlights

- Rate of oxidative addition showed little or no change with a solvent variation
- Activation volumes were determined in four of the solvents, which varied between +10.2(9) for chloroform to -18(1) cm³mol⁻¹ for acetonitrile.
- Solvent variation obeyed the Kirkwood equation with an intrinsic volume of activation of -21(3) cm³.
- DFT analysis of the oxidative addition reaction confirmed that the *trans* addition product is energetically and more stable than the four possible *cis* products.